

A Numerical Study of Fluid Flow in the Porous Structure of Biological Scaffolds

Ch. Daulbayev^{1,2,3}, Z. Mansurov^{1,2}, F. Sultanov^{1,2*}, M. Shams^{1,2}, A. Umirzakov³, S. Serovajsky¹

¹Al-Farabi Kazakh National University, 71 Al-Farabi ave., Almaty, Kazakhstan

²Institute of Combustion Problems, 172 Bogenbay batyr str., Almaty, Kazakhstan

³Satbayev University, 22a Satpaev str., Almaty, Kazakhstan

Article info

Received:
13 January 2020

Received in revised form:
2 April 2020

Accepted:
12 June 2020

Keywords:

Biologically soluble scaffolds
Tissue engineering
Fluid flow
3D printing

Abstract

Tissue engineering (TE) is one of the promising areas that aims to address the global problem of organ and tissue shortages. The successful development of TE, particularly in bone tissue engineering, consists of the use of modern methods that allow the creation of scaffolds, the physicochemical, mechanical, and structural parameters of which will allow achieving the desired clinical results. The vast possibilities of the rapidly developing technology of three-dimensional (3D) printing, which allows the creation of individual scaffolds with high precision, has led to various developments in bone tissue TE. In this work, for the successful use of three-dimensional printing in TE to ensure the diffusion of nutrients during cell cultivation throughout the entire structure of the scaffold, a model of a rotating scaffold is proposed, and the movement of the diffusion flow of nutrient fluid is calculated based on Darcy's law, which regulates the flow of fluids through porous media. The conducted studies of the rate of diffusion flow of nutrients based on glucose in the porous structure of scaffolds with a 10% content of calcium hydroxyapatite demonstrated the promise of using a model of a rotating composite scaffold in TE of bone tissue. The results show that at a scaffold rotation speed of 12 rpm, the diffusion flow rate of nutrients in the composite scaffolds porous structure is practically not affected by their geometric shape.

1. Introduction

Tissue engineering (TE) is a field of regenerative medicine, which is aimed at the development and application of various methods and principles of scientific areas such as biology, materials science, nanotechnology and medicine, allowing to obtain biological surrogates for the restoration or replacement of damaged areas of human organs or tissues [1–3]. Despite the active development of TE in the last few decades, some problems remain unsolved, namely: the high cost of an artificial organ growing [4]; difficult achievement of cell distribution with high density [5] and spatial position accuracy [6]; as well as the achievement of oriented growth of blood vessels [7].

On the other hand, the use of 3D printing tech-

nology in TE will not only solve the existing difficulties, but also may lead to significant progress in the field of regenerative medicine, due to some reasons such as the simplicity of 3D printing technology; the ability to create objects with a unique individual geometric shape; precision manufacturing of parts; the possibility of using various types of materials [8–10].

Today, the use of 3D printing in the field of medicine has a general name – bioprinting and includes the manufacture of implants [11] and biological scaffolds for growing organs and tissues [12], testing drugs [13], as well as direct printing of organs [14]. Unlike traditional methods used in 3D printing technology, materials in bioprinting are mainly presented by cells, biological materials and nutrients that stimulate cell growth. By using this process an artificial tissue with a very precise structure of the human organ can be accurately

*Corresponding author. E-mail: fail_23@bk.ru

created and thereby the main problem of TE can be solve. Bioprinting technology has incomparable advantages, especially for heterogeneous tissue which is constructed by using multiple types of cell. In the past few years, bioprinting has made tremendous progress in many aspects, such as computer modeling of organs and blood vessels, and printing techniques have improved significantly.

Among the possible applications of bioprinting in TE, the fabrication of biological scaffolds is a promising area of scientific investigations, which includes the printing of porous structures that can be seeded with autologous cells for growing cellular structures of a tissue or an organ [15–17]. For example, by combining biomaterials, culture conditions and cells, strategies can ultimately be found for producing synthetic bone transplants that can provide both the initial mechanical support for cellular structures and the necessary osteoconductive/inductive and angiogenic interactions at the site of bone repair. However, one of the main limitations in the use of scaffolds fabricated by bioprinting technology is the limitations associated with cell migration and tissue growth in these structures [18]. Since cells located in the inner scaffold receive nutrients only through diffusion from the environment in static culture, the high cell density on the outer surface of the scaffold can deplete nutrient supply before these nutrients can diffuse into the central portion of the scaffold to support tissue growth.

In order to avoid possible restrictions on the transfer of nutrients in the resulting biological scaffold, a rotating scaffold model was proposed in the current work to ensure the diffusion of nutrients during cell cultivation. Polycaprolactone (PCL) polymer and calcium hydroxyapatite (HAP) powder were chosen as the scaffold materials to study the parameters of the movement of glucose-based nutrient fluid in the porous structure of the biological scaffold. PCL is biodegradable, non-immunogenic, non-carcinogenic and non-toxic polymer with excellent biocompatibility, and due to that it can be used for obtaining composite films, which are widely applied in the TE field. Its chemical and biological properties, such as biological compatibility and mechanical strength, make it possible to use it in the implantation of bone tissues in the body, where healing also takes a long period. The use of HAP particles as part of a composite biological scaffold is due to the maintenance of migration, proliferation, and differentiation of cells and the bonding of these cells to the scaffold.

2. Material and methods

Mathematical calculations for determining the rate of diffusion flow of nutrients based on glucose were carried out using the MATLAB software, using various interfaces and packages. Partial codes were taken from [19], which describes fluid dynamics in a porous medium, and the results were verified using OpenFOAM software.

All received data were processed and analyzed using the JMP IN 15 software (Al-Farabi Kazakh National University, Almaty, Kazakhstan).

All models are modeled using Trimble SketchUp 2020. Preparation and modification for 3D printing are done by Autodesk Netfabb 2020.

3. Result and discussions

3.1. Numerical simulation of the nutrient fluid flow

For the successful application of a composite scaffold based on polymer and HAP, calculations of the movement of a nutrient fluid based on glucose in a porous structure were carried out on the basis of a mathematical model, the fundamental and theoretical aspects of which were described in detail in [20–22]. The model is based on Darcy's law, which regulates the flow of fluids through porous media and was formulated by the French civil engineer Henry Darcy in 1856 on the basis of his experiments on vertical filtration of water through sandy layers. For the movement of nutrient fluid in the porous structure of the scaffold it is presented by the equation [23]:

$$U = -\frac{K}{\eta} \nabla P, \quad (1)$$

where U is the rate of diffusion flow of nutrients (filtration rate) through the scaffold, K is the permeability through the porous medium of the biological scaffold (Darcy's permeability constant), η is the dynamic viscosity of the nutrient fluid (at 23 °C), ∇P is the pressure gradient (Fig. 1).

Parametric analysis of fluid perfusion through the scaffold was performed depending on the pore size, pore volume, and geometry of the scaffold channels. To assess the diffusion rate of nutrients in biological scaffolds, the considered model of glucose diffusion has the following assumptions:

1. The biological scaffold is permeable to the flow of nutrient fluid;

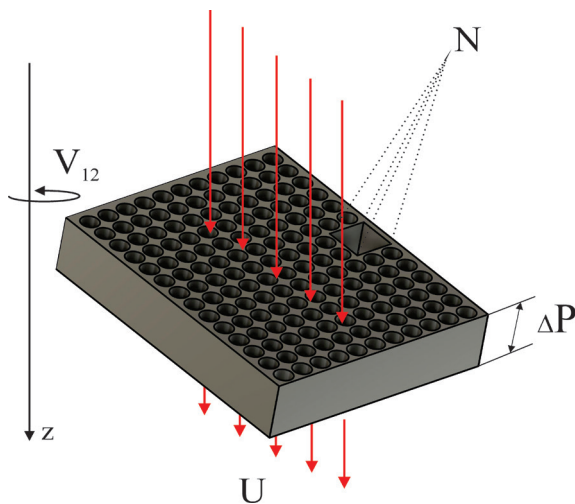


Fig. 1. Schematic representation of the movement of the nutrient fluid in the porous structure of the scaffold: U is the rate of diffusion flow of nutrients through the scaffold, V_{12} is the rotation rate of the biological scaffold, N is the unit volume of the scaffold, ΔP is the pressure difference before and after the passage of the nutrient fluid.

2. P is approximately equal to the pressure difference per unit length of the scaffold (Fig. 1), while the pressure difference is determined according to [24]:

$$\frac{\Delta P}{L} = \frac{F}{N}, \quad (2)$$

where N is the unit volume of the scaffold, L is the length of the scaffold, F is the force of resistance to the movement of nutrients, represented by the expression [24]:

$$F = \frac{4\pi\eta V_{12} R}{\ln\left(\frac{2R}{L}\right) - 0.72}, \quad (3)$$

where R is the radius of the scaffold, V_{12} is the rotation rate of the biological scaffold.

The mass flow of the glucose-based nutrient fluid was determined from the density and velocity of the fluid with the boundary region and the direction of flow. It should be noted, that to simulate a real experiment, the rate of diffusion flow of nutrients was chosen in only one direction. Wherein, the following assumption that the flow is uniform was applied, i.e. the fluid velocity is constant. Along with this, the fluid pressure at the inlet and outlet, which determine ΔP , is directed along the normal to the boundary (along the direction of the flow of the nutrient fluid, Fig. 1), while for each selected

scaffold, its boundary conditions were considered, which depend on its geometric shape, pore sizes and the initial flow rate of the liquid, that in our case was 0.5 and 1 ml/h. A detailed analysis of the boundary conditions of the inlet and outlet pressure is presented in experimental works [25–27].

The permeability through the porous medium of the biological scaffold or the Darcy permeability constant was determined from the following equation [28]:

$$K = \frac{\varepsilon^3 d^2}{150(1-\varepsilon)^2}, \quad (4)$$

where ε is the porosity of the structure of scaffold, d is the diameter of the scaffold (for calculations the models cylindrical shape scaffolds were selected for the convenience to simulate fluid motion, also taking into account the fact, that mainly cylindrical shape models of scaffolds for TE are commonly used).

The initial conditions of the modeling process are the following: physical parameters of the scaffold such as length, radius and pore size were used in Eqs. 1–4 to determine the rate of diffusion of nutrient fluid through it. To take into account the effect of the structure of the scaffolds, the parameter of the unit volume of the scaffold (N), presented in Eq. 2, was introduced. In addition, an aqueous solution of glucose (47%) was selected as the nutrient fluid, according to the tabular data, the viscosity for this percentage of glucose is 18.3 cP. It is important to note that the viscosity of a saturated glucose solution depends on the ambient temperature. As the temperature rises, the viscosity rises, and for our modeling process the ambient temperature was 20 °C.

3.2. Results of internal flow modeling

In previous studies, we have shown that HAP has a positive effect on migration, proliferation, and differentiation of cells and their bonding to scaffold, which was prepared in the form of a matrix based on polymer nanosized fibers with the addition of HAP particles [29–34]. Based on the obtained in our studies results, as well as on the studies carried out in experimental works devoted to the study of biological scaffolds [35–37], fabricated by 3D printing technology, we modeled composite scaffolds with different types of structures, and the significant difference between the indicated above studies and our model was the

content of HAP, which in our scaffolds did not exceed 10%. According to [38] the presence of HAP in the scaffold structure over 10% adversely affects its mechanical properties.

To study the rate of diffusion flow of nutrients in a porous structure, well-proven in TE scaffolds were selected (Fig. 2), the parameters of which are described in Table.

The table presents the physical parameters of the simulated scaffolds, according to which their average pore size is in the range from 3 to 7 mm, while their masses are comparable, the average

mass is 8.213 ± 0.13 g. Obviously, the geometric shape and pore sizes affect the porosity of the entire scaffold structure, and according to the calculations, the average porosity value is 0.705 ± 0.06 . The measurement of the values of the volume fraction of voids for all types of scaffold structures varied from 64 to 76%, which is consistent with the data presented in experimental works [39–42].

Figure 3 shows the results of numerical simulation of the rate of diffusion flow of nutrients based on glucose in the porous structure of different types of scaffolds. It should be noted that the

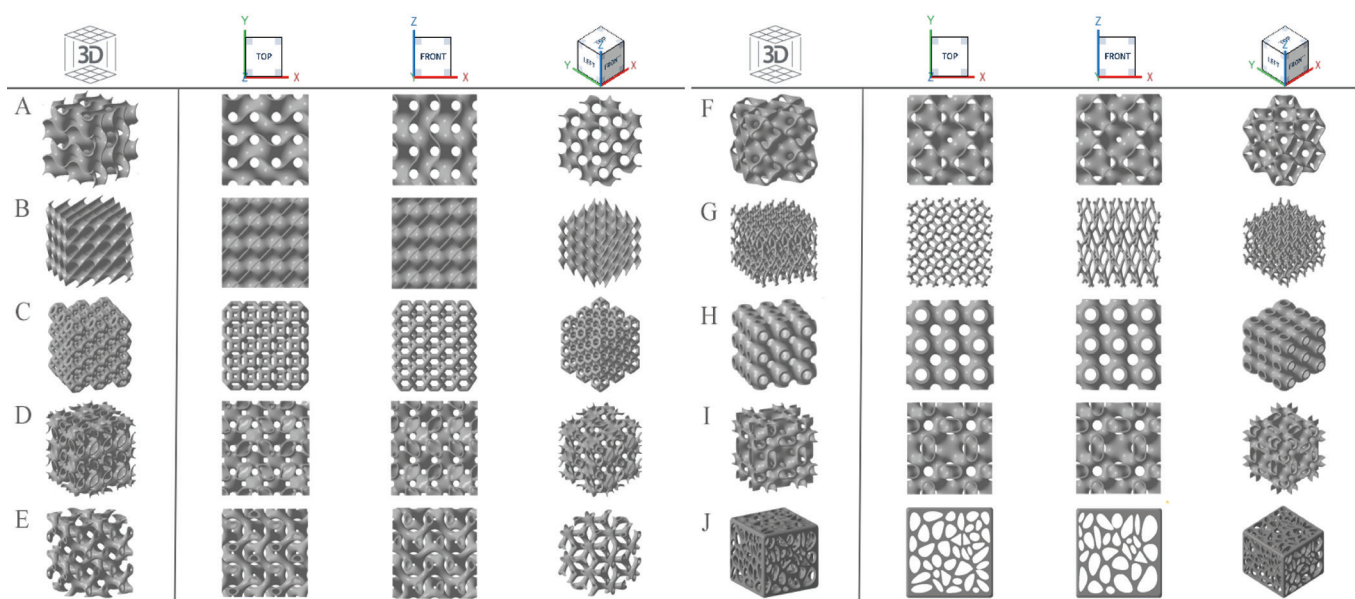


Fig. 2. Different types of modeled scaffolds (Description of the types of structures and their parameters are presented in Table).

Table
Parameters of biological scaffolds

Sample	Inspired/Mathematical Structure	Dimension (L. W. H)/(mm)	Average Pore Size/(mm)	Porosity	Weight/(gr)	Mass Fraction (HAp/PCL)
A	Gyroid Membrane structure	25.25.25	5.44	~0.70	8.34	0.1/0.9
B	Customized structure	25.25.25	3.92	~0.60	8.68	0.1/0.9
C	Kelvin lattice (weaire–phelan)	25.25.25	5.48	~0.70	8.13	0.1/0.9
D	Lidinoïd structure	25.25.25	4.88	~0.65	8.33	0.1/0.9
E	Nodal structure	25.25.25	6.26	~0.75	7.89	0.1/0.9
F	Customized Octo-structure	25.25.25	4.34	~0.65	8.45	0.1/0.9
G	Customized structure	25.25.25	4.12	~0.80	7.81	0.1/0.9
H	Schwarz P structure	25.25.25	5.34	~0.75	8.04	0.1/0.9
I	Customized structure	25.25.25	4.98	~0.75	8.19	0.1/0.9
J	Voronoi Diagram	25.25.25	4.64	~0.70	8.27	0.1/0.9

graphs were constructed using cubic data interpolation, while the calculations were carried out for scaffold rotation rates from 1 to 24 rpm with a single step.

As can be seen from Fig. 2, for each type of scaffold (see Table), the rate of diffusion flow of nutrients increases with the increase of the rate of its rotation. However, for scaffolds of type B, C, E, F, G (Fig. 2b), there is a linear increase in the rate of liquid diffusion up to 5 ml/h at 12 rpm, after which a constant value is set for scaffolds E, F and G, while for scaffolds B and C a uniform decrease is observed.

For scaffolds A, D, H, I and J, the rate of diffusion flow of nutrients is higher, with the maximum value of 10.89 ml/h for scaffold I. The linear growth is observed up to a diffusion rate of 8–9 ml/h with a scaffold rotation rate of 16–18 rpm. Presumably, for these types of scaffolds, the current dependence will also reach a level at which the rates of diffusion of nutrients through the scaffold will not be determined by their rotation rates. At the same time, the results obtained within the scaffolds of the presented model of composite biological scaffolds with 10% of HAP content and the studied pore architecture, are consistent with experimental observations of bone tissue growth in three-dimensional scaffolds [21, 43–45] which present a quantitative assessment of the rate of diffusion flow of nutrients at culturing cells (*in vitro*) with high density. Although the model has some assumptions, studies have shown that physical parameters such as total pore volume and pore diameter have a significant impact on the internal perfusion of nutrients.

The influence of the average pore size on the movement of the nutrient fluid through the scaffold

is presented in Fig. 4, wherein three values of the rotation rate (6, 12, 24 rpm) were selected, for which the diffusion rates of the nutrient fluid depending on their average pore size (Table) were studied.

The values of the rate of diffusion flow of nutrients depending on the average pore size of the scaffold, which is in the range from 3.92 to 6.26 mm (Table) at a certain rotation rate, showed that the geometric shape of the scaffold has a significant effect on the movement of the nutrient fluid. For the G and E scaffold, the average pore size is 4.12 and 6.26 mm, respectively, but for both scaffolds the rate of diffusion flow of nutrients is approximately the same – 2.8 ml/h (Fig. 4a). A detailed study of the effect of the average pore size of scaffolds on the rate of diffusion flow of nutrients through it at 12 rpm (Fig. 3b) indicates that the pores do not significantly affect the rate of nutrient spread. Such behavior at similar parameters is confirmed in experimental works [42, 46–48] and possibly indicates the selection of the optimal scaffold rotation rate. At rotation rates of 24 rpm (Fig. 4c) and 6 rpm (Fig. 4a), the influence of the geometric shape on the distribution of the nutrient in the scaffold is clearly seen.

Despite the fact that the performed numerical modeling requires direct *in vitro* analysis for a detailed study of the influence of the shape and pore size of scaffolds, the type of nutrient and its composition, on the growth of cells, our studies are in agreement with a number of works [49–51]. Moreover, the numerical results of our studies on the rate of diffusion flow of nutrients at a certain rate of rotation of the scaffold were lower than the actual rate of particle movement, observed in these works.

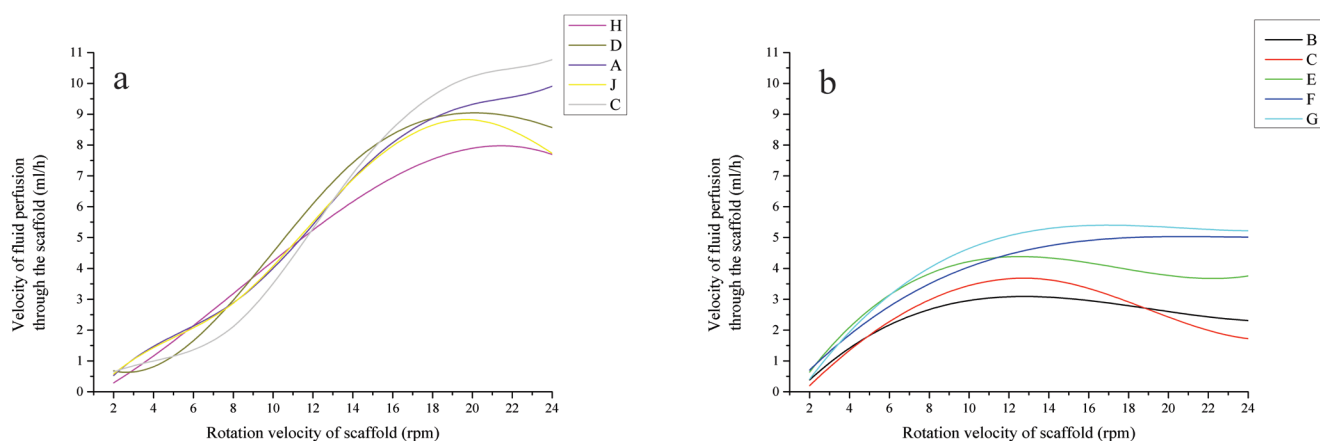


Fig. 3. Dependence of the rate of diffusion of nutrients through the scaffolds on the rate of its rotation for scaffolds A, D, H, I, J (a) and for scaffolds B, C, E, F, G (b).

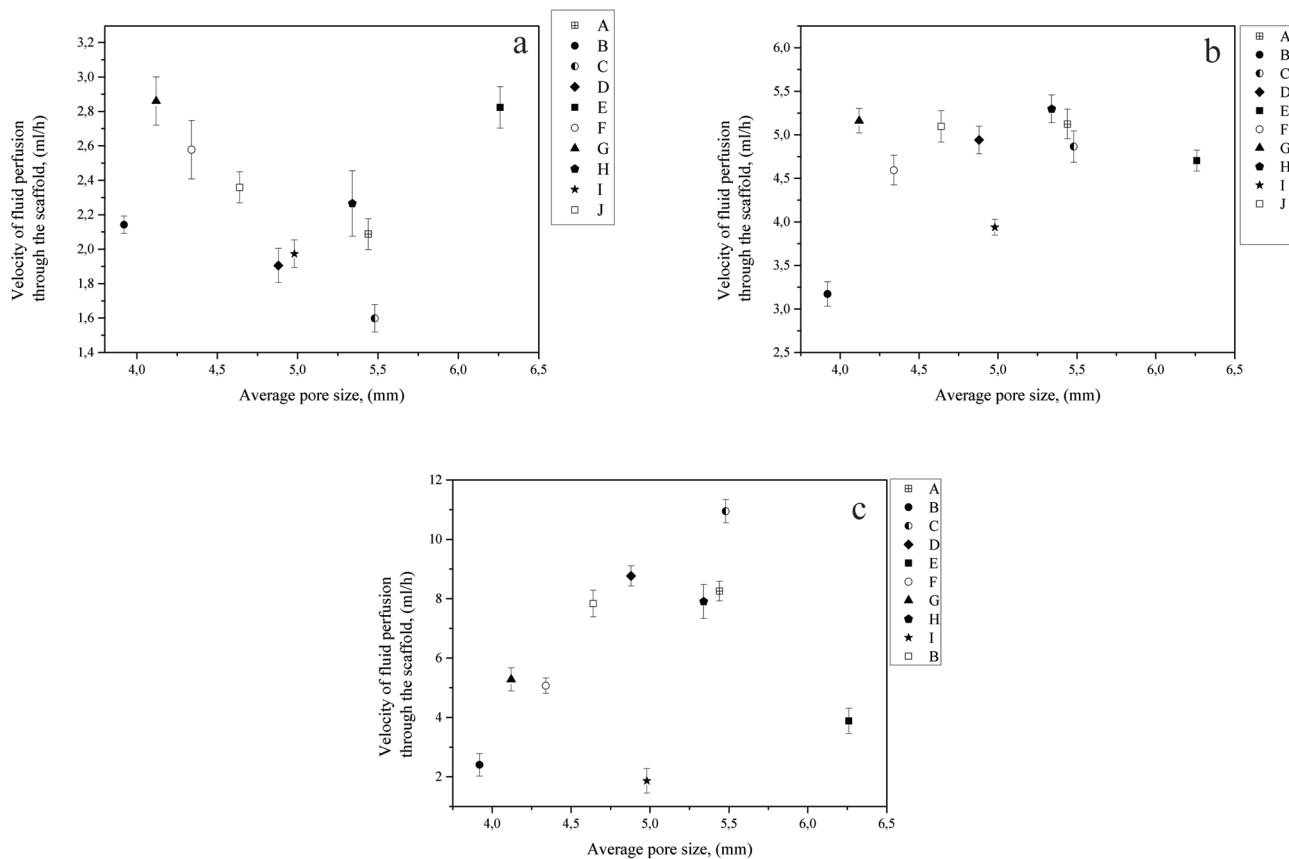


Fig. 4. Influence of the average pore size on the rate of diffusion of nutrient fluid through the scaffold at its rotation rate of 6 (a), 12 (b) and 24 (c) rpm.

Based on theoretical and practical investigations, in our study, for the first time, a quantitative assessment of the values of the rate of diffusion flow of nutrients fluids based on glucose in the structure of three-dimensional porous composite scaffolds with different geometric shapes and addition of HAP, was conducted. As a result, the optimal rotation rate of the scaffold was determined at which the rate of diffusion flow of nutrients is practically independent of its shape, and the obtained data can be used for future research in the field of TE. Obviously, all the assumptions underlying our model used in calculating the rate of nutrient diffusion do not fully reflect the complex hydrodynamic process of fluid movement in a three-dimensional structure. Nevertheless, the complex process of studying the diffusion of fluid and the profile of the internal flow of nutrient fluid in the biological scaffold is the subject of our future studies, including the *in vitro* investigations.

4. Conclusion

A glucose-based nutrient flow study using a theoretical model based on Darcy's law provided a quantitative assessment of the use of compos-

ite biological scaffolds with the addition of HAP in the field of tissue engineering of bone tissue. Studies have shown that the use of a rotating scaffold model in TE of bone tissue for growing cell structures is one of the possible solutions to insufficient cell migration and tissue growth in these structures *in vivo* and *in vitro*. Based on the results of a numerical study, it has been shown that at a scaffold rotation speed of 12 rpm, the scaffold's geometric shape has practically no effect on the rate of diffusion flow of nutrients based on glucose. Also, based on the results obtained in this work, a method is being developed to determine the behavior of cellular structures in a biological framework for further *in vitro* studies.

Acknowledgements

The authors thank prof. Kaltayev A.Zh. for valuable consultations and discussion of the results obtained.

References

- [1]. M.S. Hall, J.T. Decker, L.D. Shea, *Biomaterials* 255 (2020) 120189. DOI: [10.1016/j.biomaterials.2020.120189](https://doi.org/10.1016/j.biomaterials.2020.120189)

- [2]. C. Li, L. Ouyang, J.P.K. Armstrong, M.M. Stevens, *Trends Biotechnol.* (2020) In press. DOI: [10.1016/j.tibtech.2020.06.005](https://doi.org/10.1016/j.tibtech.2020.06.005)
- [3]. I.M. Zurina, V.S. Presniakova, D.V. Butnaru, A.A. Svistunov, P.S. Timashev, Y.A. Rochev, *Acta Biomater.* 113 (2020) 63–83. DOI: [10.1016/j.actbio.2020.06.016](https://doi.org/10.1016/j.actbio.2020.06.016)
- [4]. M.T. Calejo, T. Ilmarinen, H. Skottman, M. Kellomäki, *Acta Biomater.* 66 (2018) 44–66. DOI: [10.1016/j.actbio.2017.11.043](https://doi.org/10.1016/j.actbio.2017.11.043)
- [5]. S. Pina, V.P. Ribeiro, O.C. Paiva, V.M. Correlo, J.M. Oliveira, R.L. Reis, *Handbook of Tissue Engineering Scaffolds: Volume One*, 2019, pp. 165–185. DOI: [10.1016/B978-0-08-102563-5.00009-5](https://doi.org/10.1016/B978-0-08-102563-5.00009-5)
- [6]. M.E. Furth, A. Atala, *Principles of Tissue Engineering (Fourth Edition)*, 2014, pp. 83–123. DOI: [10.1016/B978-0-12-398358-9.00006-9](https://doi.org/10.1016/B978-0-12-398358-9.00006-9)
- [7]. Q. Fu, E. Saiz, M.N. Rahaman, A.P. Tomsia, *Mater. Sci. Eng. C* 31 (2011) 1245–1256. DOI: [10.1016/j.msec.2011.04.022](https://doi.org/10.1016/j.msec.2011.04.022)
- [8]. A. Haleem, M. Javaid, R.H. Khan, R. Suman, *J. Clin. Orthop. Trauma* 11 (2020) S118–S124. DOI: [10.1016/j.jcot.2019.12.002](https://doi.org/10.1016/j.jcot.2019.12.002)
- [9]. C. Wang, W. Huang, Y. Zhou, L. He, Z. He, Z. Chen, X. He, S. Tian, J. Liao, B. Lu, Y. Wei, M. Wang, *Bioact. Mater.* 5 (2020) 82–91. DOI: [10.1016/j.bioactmat.2020.01.004](https://doi.org/10.1016/j.bioactmat.2020.01.004)
- [10]. J. Zhang, S. Yun, A. Karami, B. Jing, A. Zannettino, Y. Du, H. Zhang, *Bioprinting* 19 (2020) e00089. DOI: [10.1016/j.bprint.2020.e00089](https://doi.org/10.1016/j.bprint.2020.e00089)
- [11]. C.-H. Li, C.-H. Wu, C.-L. Lin, *J. Mech. Behav. Biomed. Mater.* 105 (2020) 103700. DOI: [10.1016/j.jmbbm.2020.103700](https://doi.org/10.1016/j.jmbbm.2020.103700)
- [12]. L. Wei, S. Wu, M. Kuss, X. Jiang, R. Sun, P. Reid, X. Qin, B. Duan, *Bioact. Mater.* 4 (2019) 256–260. DOI: [10.1016/j.bioactmat.2019.09.001](https://doi.org/10.1016/j.bioactmat.2019.09.001)
- [13]. S. Beg, W.H. Almalki, A. Malik, M. Farhan, M. Aatif, K.S. Alharbi, N.K. Alruwaili, M. Alrobaian, M. Tarique, M. Rahman, *Drug Discov. Today* (2020) In press. DOI: [10.1016/j.drudis.2020.07.007](https://doi.org/10.1016/j.drudis.2020.07.007)
- [14]. S. Liu, H. Zhang, Q. Hu, Z. Shen, D. Rana, M. Ramalingam, *J. Mech. Behav. Biomed. Mater.* 104 (2020) 103642. DOI: [10.1016/j.jmbbm.2020.103642](https://doi.org/10.1016/j.jmbbm.2020.103642)
- [15]. C.Q. Zhao, X.C. Xu, Y.J. Lu, S.Q. Wu, Z.Y. Xu, T.T. Huang, J.X. Lin, *J. Alloy. Compd.* 814 (2020) 152327. DOI: [10.1016/j.jallcom.2019.152327](https://doi.org/10.1016/j.jallcom.2019.152327)
- [16]. W. Zhang, I. Ullah, L. Shi, Y. Zhang, H. Ou, J. Zhou, M.W. Ullah, X. Zhang, W. Li, *Mater. Design* 180 (2019) 107946. DOI: [10.1016/j.matdes.2019.107946](https://doi.org/10.1016/j.matdes.2019.107946)
- [17]. N.M. Ergul, S. Unal, I. Kartal, C. Kalkandelen, N. Ekren, O. Kilic, L. Chi-Chang, O. Gunduz, *Polymer Test.* 79 (2019) 106006. DOI: [10.1016/j.polymertesting.2019.106006](https://doi.org/10.1016/j.polymertesting.2019.106006)
- [18]. G.E. Dubinenko, A.L. Zinoviev, E.N. Bolbasov, V.T. Novikov, S.I. Tverdokhlebov, *Mater. Today: Proc.* 22 (2020) 228–234. DOI: [10.1016/j.matpr.2019.08.092](https://doi.org/10.1016/j.matpr.2019.08.092)
- [19]. A. Nakayama, I. Pop, *Int. J. Heat and Mass Tran.* 34 (1991) 357–367. DOI: [10.1016/0017-9310\(91\)90256-E](https://doi.org/10.1016/0017-9310(91)90256-E)
- [20]. G. Fragomeni, R. Iannelli, G. Falvo D’Urso Labate, M. Schwentenwein, G. Catapano, *New Biotechnol.* 52 (2019) 110–120. DOI: [10.1016/j.nbt.2019.06.001](https://doi.org/10.1016/j.nbt.2019.06.001)
- [21]. S. Grossemy, P.P.Y. Chan, P.M. Doran, *Biochem. Eng. J.* 159 (2020) 107602. DOI: [10.1016/j.bej.2020.107602](https://doi.org/10.1016/j.bej.2020.107602)
- [22]. P. Kumar, B. Dey, G.P. Raja Sekhar, *Int. J. Eng. Sci.* 127 (2018) 201–216. DOI: [10.1016/j.ijengsci.2018.02.013](https://doi.org/10.1016/j.ijengsci.2018.02.013)
- [23]. I.I. Krashin, L.V. Semendyaeva, A.I. Zinin, G.A. Zinina. *Elsevier Geo-Engineering Book Series 2* (2004) 679–684. DOI: [10.1016/S1571-9960\(04\)80118-6](https://doi.org/10.1016/S1571-9960(04)80118-6)
- [24]. E.A. Botchwey, S.R. Pollack, E.M. Levine, E.D. Johnston, C.T. Laurencin, *J. Biomed. Mater. Res. A* 69A (2004) 205–215. DOI: [10.1002/jbm.a.10163](https://doi.org/10.1002/jbm.a.10163)
- [25]. L.V. Gonzalez Gil, H. Singh, J. de Sa. da Silva, D.P. dos Santos, D.T. Covas, K. Swiech, C.A. Torres Suazo, *Biochem. Eng. J.* 162 (2020) 107710. DOI: [10.1016/j.bej.2020.107710](https://doi.org/10.1016/j.bej.2020.107710)
- [26]. B.S. Borys, A. Le, E.L. Roberts, T. Dang, L. Rohani, C.Y.-M. Hsu, A.A. Wyma, D.E. Rancourt, I.D. Gates, M.S. Kallos, *J. Biotechnol.* 304 (2019) 16–27. DOI: [10.1016/j.jbiotec.2019.08.002](https://doi.org/10.1016/j.jbiotec.2019.08.002)
- [27]. P. Yu, T.S. Lee, Y. Zeng, H.T. Low, *Int. J. Heat Mass Tran.* 52 (2009) 316–327. DOI: [10.1016/j.ijheatmasstransfer.2008.06.021](https://doi.org/10.1016/j.ijheatmasstransfer.2008.06.021)
- [28]. M. Ciofalo, M.W. Collins, T.R. Hennessy, *Med. Eng. Phys.* 18 (1996) 437–451. DOI: [10.1016/1350-4533\(95\)00081-X](https://doi.org/10.1016/1350-4533(95)00081-X)
- [29]. Ch.B. Daulbaev, T.P. Dmitriev, F.R. Sultanov, Z.A. Mansurov, E.T. Aliev, *J. Eng. Phys. Thermophy.* 90 (2017) 1115–1118. DOI: [10.1007/s10891-017-1665-z](https://doi.org/10.1007/s10891-017-1665-z)
- [30]. Ch. Daulbayev, Z. Mansurov, G. Mitchell, A. Zakhidov, *Eurasian Chem.-Technol. J.* 20 (2018) 119–124. DOI: [10.18321/ectj690](https://doi.org/10.18321/ectj690)
- [31]. F. Sultanov, C. Daulbayev, B. Bakbolat, O. Daulbayev, M. Bigaj, Z. Mansurov, K. Kuterbekov, K. Bekmyrza, *Chem. Phys. Lett.* 737 (2019) 136821. DOI: [10.1016/j.cplett.2019.136821](https://doi.org/10.1016/j.cplett.2019.136821)
- [32]. F. Sultanov, B. Bakbolat, Z. Mansurov, Z. Azizov, S.-S. Pei, R. Ebrahim, C. Daulbayev, A. Urazgaliyeva, M. Tulepov, *Eurasian Chem.-Technol. J.* 19 (2017) 127–132. DOI: [10.18321/ectj286](https://doi.org/10.18321/ectj286)
- [33]. F.R. Sultanov, C. Daulbayev, B. Bakbolat, Z.A.

- Mansurov, A.A. Urazgaliyeva, R. Ebrahim, S.S. Pei, K.-P. Huang, *Carbon Lett.* 30 (2020) 81–92. DOI: [10.1007/s42823-019-00073-5](https://doi.org/10.1007/s42823-019-00073-5)
- [34]. F.R. Sultanov, Ch. Daulbayev, B. Bakbolat, Z.A. Mansurov, *Eurasian Chem.-Technol. J.* 20 (2018) 195–200. DOI: [10.18321/ectj721](https://doi.org/10.18321/ectj721)
- [35]. D.A. Zopf, C.L. Flanagan, A.G. Mitsak, J.R. Brennan, S.J. Hollister, *Int. J. Pediatr. Otorhi.* 114 (2018) 170–174. DOI: [10.1016/j.ijporl.2018.07.033](https://doi.org/10.1016/j.ijporl.2018.07.033)
- [36]. M. Hemshekhar, R.M. Thushara, S. Chandranayaka, L.S. Sherman, K. Kemparaju, K.S. Girish, *Int. J. Biol. Macromol.* 86 (2016) 917–928. DOI: [10.1016/j.ijbiomac.2016.02.032](https://doi.org/10.1016/j.ijbiomac.2016.02.032)
- [37]. M. Milojević, L. Gradišnik, J. Stergar, M. Skelin Klemen, A. Stožer, M. Vesenjāk, P. Dobnik Dubrovski, T. Maver, T. Mohan, K. Stana Kleinschek, U. Maver, *Appl. Surf. Sci.* 488 (2019) 836–852. DOI: [10.1016/j.apsusc.2019.05.283](https://doi.org/10.1016/j.apsusc.2019.05.283)
- [38]. M.U.A. Khan, S. Haider, S.A. Shah, S.I.A. Razak, S.A. Hassan, M.R.A. Kadir, A. Haider, *Int. J. Biol. Macromol.* 151 (2020) 584–594. DOI: [10.1016/j.ijbiomac.2020.02.142](https://doi.org/10.1016/j.ijbiomac.2020.02.142)
- [39]. M. Ramadas, K. ElMabrouk, A.M. Ballamurugan, *Mater. Chem. Phys.* 242 (2020) 122456. DOI: [10.1016/j.matchemphys.2019.122456](https://doi.org/10.1016/j.matchemphys.2019.122456)
- [40]. B.W.M. de Wildt, S. Ansari, N.A.J.M. Sommerdijk, K. Ito, A. Akiva, S. Hofmann, *Curr. Opin. Biomed. Eng.* 10 (2019) 107–115. DOI: [10.1016/j.cobme.2019.05.005](https://doi.org/10.1016/j.cobme.2019.05.005)
- [41]. C.M. Agrawal, J.S. McKinney, D. Lanctot, K.A. Athanasiou, *Biomaterials* 21 (2000) 2443–2452. DOI: [10.1016/S0142-9612\(00\)00112-5](https://doi.org/10.1016/S0142-9612(00)00112-5)
- [42]. D. Ali, M. Ozalp, S.B.G. Blanquer, S. Onel, *Eur. J. Mech. B-Fluid.* 79 (2020) 376–385. DOI: [10.1016/j.euromechflu.2019.09.015](https://doi.org/10.1016/j.euromechflu.2019.09.015)
- [43]. H. Seddiqi, A. Saatchi, G. Amoabediny, M.N. Helder, S.A. Ravasjani, M.S. Hajat Aghaei, J. Jin, B. Zandieh-Doulabi, J. Klein-Nulend, *Comput. Biol. Med.* 24 (2020) 103826. DOI: [10.1016/j.compbiomed.2020.103826](https://doi.org/10.1016/j.compbiomed.2020.103826)
- [44]. M. Malvè, D.J. Bergstrom, X.B. Chen, *Int. Commun. Heat Mass Trans.* 96 (2018) 53–60. DOI: [10.1016/j.icheatmasstransfer.2018.05.014](https://doi.org/10.1016/j.icheatmasstransfer.2018.05.014)
- [45]. J. Zvicer, A. Medic, D. Veljovic, S. Jevtic, S. Novak, B. Obradovic, *Polymer Test.* 76 (2019) 464–472. DOI: [10.1016/j.polymertesting.2019.04.004](https://doi.org/10.1016/j.polymertesting.2019.04.004)
- [46]. G. Belgheisi, M.H. Nazarpak, M.S. Hashjin, *Appl. Clay Sci.* 185 (2020) 105434. DOI: [10.1016/j.clay.2019.105434](https://doi.org/10.1016/j.clay.2019.105434)
- [47]. A. Abdal-hay, N.T. Raveendran, B. Fournier, S. Ivanovski, *Compos. Part B-Eng.* 197 (2020) 108158. DOI: [10.1016/j.compositesb.2020.108158](https://doi.org/10.1016/j.compositesb.2020.108158)
- [48]. J. Mesquita-Guimarães, L. Ramos, R. Detsch, B. Henriques, M.C. Fredel, F.S. Silva, A.R. Boccaccini, *J. Eur. Ceram. Soc.* 39 (2019) 2545–2558. DOI: [10.1016/j.jeurceramsoc.2019.01.029](https://doi.org/10.1016/j.jeurceramsoc.2019.01.029)
- [49]. B. Pasha Mahammad, E. Barua, A.B. Deoghare, K.M. Pandey, *Mater. Today: Proc.* 22 (2020) 1687–1693. DOI: [10.1016/j.matpr.2020.02.186](https://doi.org/10.1016/j.matpr.2020.02.186)
- [50]. S. Pathmanapan, P. Periyathambi, S.K. Anandasadagopan, *Nanomed: Nanotechnol. Biol. Med.* 29 (2020) 102251. DOI: [10.1016/j.nano.2020.102251](https://doi.org/10.1016/j.nano.2020.102251)
- [51]. S.F. Robertson, S. Bose, *J. Mech. Behav. Biomed. Mater.* (2020) 103945. DOI: [10.1016/j.jmbbm.2020.103945](https://doi.org/10.1016/j.jmbbm.2020.103945)